Development and experimental verification of a model for an air jet penetrated by plumes

Xin Wang, Yuntian Dai and Jingsi Ma

Abstract

This article presents the fluid mechanics of a ventilation system formed by a momentum source and buoyancy sources. We investigate the interaction between plumes and a non-isothermal air jet for separate sources of buoyancy produced by the plume and the momentum of the air jet. The mathematical model represents the situation in which a plume rises from two heat sources causing buoyancy. The model is used to discuss the interactions involved. The effects of parameters such as the power of the source and the air-flow volume used in the mathematical-physical model are also discussed. An expression is deduced for the trajectory of the non-isothermal air jet penetrated by plumes. Experiments were also carried out to illustrate the effect on the flow of the air jet and to validate the theoretical work. The results show that the buoyancy source's efforts to baffle the descent of the cold air have even been effective in reversing the direction of the trajectory. However, increasing the distance between the plumes can reduce the effect of the plumes on the jet curve. And it is apparent that when the velocity of the air supply increases, the interference caused by the plumes can be reduced.

Keywords

Plumes, non-isothermal air jet, mathematical modeling, air stream trajectory, experiment

Introduction

The accumulation of heat in the upper part of rooms is utilized in the stratification and zoning room air-conditioning strategies.[1] The supply air devices are located in the lower zone. The temperature of the supply air is normally lower than the temperature of the room air in the controlled zone. The zone boundary should be defined high enough to get nearly all the induction air to the supply jet from the lower zone. The plume generated by the heat source penetration through the supply air jets depends on the air distribution method, locations of the plume and supply air device, plume heat power, and momentum of the supply jets. This article presents an analytical method for modeling the supply air jet penetrated by plumes for an air distribution method based on the sidewall vents.

Many sources that generate heat may be regarded as localized, for example, electrical equipment (including computers) and occupants. The plume generated by a localized heat source at floor level in an air-conditioned space can be of considerable interest with regard to building ventilation. In this article, these sources are classified as pure buoyancy sources (characterized by

Department of Environment and Architecture, University of Shanghai for Science and Technology, Shanghai, China

Corresponding author:
Xin Wang, Department of Environment and Architecture, University of Shanghai for Science and Technology, 516 Jungong Road, Shanghai 200093, China.
Email: wangxinshiyun@126.com

zero initial momentum flux), consisting of two plumes with either the same or different power.

A constant buoyancy flux may act against the descent of the cold air produced by the jet diffuser. As a result, the temperature of the residential zone may become higher than the intended value. In addition, the temperature in the confined spaces in the upper region may be actually lower than planned as cold air lingers there. In this case, it is obvious that flow resistance between the buoyancy source (the plume) and the momentum source (the air jet) has an effect on the flowing action of the non-isothermal air jet from the air-conditioning system. This thermal buoyancy effect may raise the air jet trajectory. Therefore, the effect of heat sources on the non-isothermal jet may not be insignificant. The universal mathematical model for non-isothermal air jets includes the buoyancy force caused by the temperature difference between the indoor air and the cooling air supplied by the jet diffuser.[2]

Both at home and abroad, the calculation method of air jet is widely found in all design manuals, mainly divided into two systems:[3] the calculation system of the former Soviet Union scholar Abramovich and computing system of the US scholar Alfred Koestel. While the calculation method of air jet in some countries in Europe, Japan, and the United States use the formulas of the same basic form as in the design manuals, the calculation formulas are similar to the Alfred Koestel system with just some different experience coefficients. Air jet mostly belongs to the multiple strands of non-isothermal confined turbulent jet motion. At present, the study is aimed at turbulent characteristics,[4] trajectory,[5] and velocity distribution[6] of jet.

These computational methods greatly facilitate the design of air-conditioning system, but it is also a widespread problem and is accurate enough, without considering the influence of indoor thermal plume of air jet.

However, the buoyancy force produced by plumes has not yet been considered. Zeldovich,[7] Batchelor,[8] and Morton et al.[9] laid the foundations for classical plume theory, a theoretical description that is elegant in its simplicity and yet encapsulates the complex turbulent engulfment of ambient fluid into the plume. The theory presented—despite its simplicity—has been very successful in describing and explaining the behavior of plumes across the wide range of scales they are observed. A number of articles have been written on turbulent plumes.[10–16] The solution procedures adopted the physical implications of these, and the scope of applying these approaches more widely to other plumes and plume-like flows is presented in these articles.

Scase et al.[17] again enriched Morton et al.'s results on the basis of the research-increasing hypothesis; obtained thermal plume buoyancy flux, mass flux, and momentum flux motion control equation; and gave its approximate solution in steady uniform environment.

Many scholars have studied the multiple plume mixing and interaction problems.[18,19] Kaye and Linden[20] greatly enriched the research contents of multiple strands of plume. They start from two strands equal and unequal plume flow, respectively, from the theoretical and experimental analysis on the mixing process and movement situation after mixing of multi-strand plume mixing into axisymmetric plume, and in the entrainment coefficient determined, calculate the mixing height of plume.

In many applications, it is not the plume itself that is of primary interest, but rather its effect on the environment as a whole. Applications in the built environment include the natural ventilation of buildings where thermal plumes rising from heat sources not only determine the thermal stratification in a room but also set the rate of ventilation and thereby the comfort of occupants. The flow induced by these plumes plays a key role in setting the pattern of air movement and within a well-designed room may give rise to a desirable cooling flow through ventilation openings.[21] In other applications, it is the stratification established by the plume that is of primary interest; plumes confined within a container may be used in an experimental context specifically to stratify an environment.[22,23]

Our oceans and atmosphere are stratified and driven by a need to understand the dispersion of chemical pollutants[24] (often released locally forming pollutant plumes), the deepening of the ocean mixed layer,[25] or indeed the analogous mixed layer in a ventilated room.[26] Several workers have given attention to the cases in which there is either an air jet or heat source. Linden et al.,[27] Linden and Cooper,[28] Hunt,[29,30] and Chen et al.[31] reported on ventilation and stratification in naturally ventilated spaces driven by heat sources. Hunt et al.[32] presented an experimental study of the thermal stratification produced by plumes and jets in enclosed spaces. Cho and Awbi[33] studied the effect of heat source location in a ventilated room. In their work, the authors used multiple regression analysis to predict the average velocity in the room and to determine the parameters that have the largest influence on the velocity. List[34] reviewed the ways in which jets and plumes interact with environmental factors.

Plume penetration through air supply jets depends on the air distribution method, the locations of the plume and the device supplying air, the heating power of the plume, and the momentum of the supply jets. This article presents an analytical method for modeling plume penetration when the air distribution method is based on a sidewall supply air jet. The purpose of the theoretical work described in this article is to develop the fluid mechanics for the ventilation system. We consider the buoyancy source required for a more efficient ventilation system and develop a better trajectory expression for the non-isothermal air jet taking into

account the effect of the plume. Experiments are also performed to test the validity of the theory presented.

Methods

Penetration model

The penetration model is based on the forces created by the air supply jet and buoyancy. The principle of the model is illustrated in Figure 1.

When the jet encounters the plume, it is impacted by the plume in a direction perpendicular to its course. Thus, the speed of the jet in the perpendicular direction changes, which leads to a change in the vertical component of the velocity of the jet, as shown in Figure 1. As the air supply temperature is different from the room temperature and the plume temperature, the resultant external force is non-zero. This leads to an offset of the jet in the vertical direction. In this article, it is assumed that the offset in the vertical direction does not change the axial symmetry of the whole jet. Thus, it is enough to study the curve of the axis when studying the motion of the whole jet.

The plume phenomenon is caused by rising warm air. An analysis of the physical mechanism[14] responsible for the plume suggests that the main driving force behind the rising plume is the temperature difference between it and the ambient air which leads to a density difference, $\rho_e - \bar{\rho}$. In this expression, ρ_e is the density of the surrounding environment and $\bar{\rho}$ is the mean plume density. It can therefore be considered that the density difference is the driving force making the plume move upward. The buoyancy force, F, acting on the jet can thus be related to this density difference

$$F = k(\rho_e - \bar{\rho}) \tag{1}$$

where k is the buoyancy force factor of the plume, which may be expressed by the equation
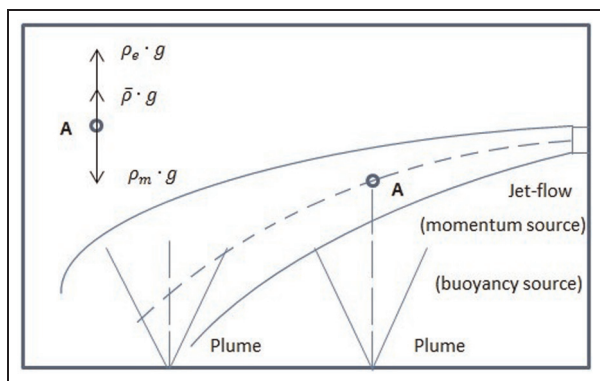

Figure 1. The interaction of the cold jet and the hot plume.

$$k = \frac{\rho_e}{(6\alpha/5)(9\alpha/10)^{1/3}F_0^{-2/3}\rho_e^{2/3}z^{5/3}g + 1}.$$

where ρ_e (kg/m^3) is the density of the environment surrounding the plume, α is the entrainment factor, F_0 (m^3/s^2) is the buoyancy flux of the plume, z (m) is the height to which the plume develops, g (m/s^2) is the acceleration due to gravity, and $\bar{\rho}$ (kg/m^3) is the average density of several plumes.

Morton et al.[9] showed that the density of the plume is related to the momentum flux, buoyancy flux, and mass flux, which can be expressed as follows

$$\rho = \rho_e \frac{gG}{gG + F} \tag{2}$$

where G (m^3/s) is the mass flux of the plume generated by the point source and F (m^4/s^3) is the buoyancy flux of the plume generated by the point source.

The density of the plume generated by the mixing of the two plumes can be represented as a function of height z:

1. Mixing of two plumes with the same power

$$\rho = \rho_e \frac{2\left(\frac{5F}{4\alpha}\right)^{1/3}\left(\frac{6\alpha z}{5}\right)^{5/3}g}{2\left(\frac{5F}{4\alpha}\right)^{1/3}\left(\frac{6\alpha z}{5}\right)^{5/3}g + 2F} \tag{3}$$

2. Mixing of two plumes with different power

$$\rho = \rho_e \frac{\left(1 + \psi^{1/3}\right)\left(\frac{5F_1}{4\alpha}\right)^{1/3}\left(\frac{6\alpha z}{5}\right)^{5/3}g}{\left(1 + \psi^{1/3}\right)\left(\frac{5F_1}{4\alpha}\right)^{1/3}\left(\frac{6\alpha z}{5}\right)^{5/3}g + \left(1 + \psi^{1/3}\right)F_1} \tag{4}$$

where ψ is the buoyancy flux ratio. Then, at height z, the average density of several plumes can be expressed as

$$\bar{\rho} = \frac{1}{z - z_m}\int_{z_m}^{z}\rho \, dz \tag{5}$$

Defining the upward direction to be positive, the external force F_1 on the unit A can be expressed as

$$F_1 = (\rho_e - \rho_m)g + F = (\rho_e - \rho_m)g + k(\rho_e - \bar{\rho}) = \rho_m j \tag{6}$$

where ρ_m (kg/m^3) is the axis density of the plume and j is the effective vertical acceleration due to gravity. This can be transformed into

$$j = \frac{(\rho_e - \rho_m)}{\rho_m}g + \frac{k(\rho_e - \bar{\rho})}{\rho_m} \tag{7}$$

According to basic physics, the relationship between the descending distance y' of the cold jet pivot, the

vertical velocity component u_y', and the vertical acceleration due to gravity j is given by

$$j = \frac{du_y'}{dt} = \frac{d^2 y'}{dt^2} \tag{8}$$

Thus

$$u_y' = \int j dt = \int \left[\frac{(\rho_e - \rho_m)}{\rho_m} g + \frac{k(\rho_e - \bar{\rho})}{\rho_m} \right] dt$$
$$= \int \frac{(\rho_e - \rho_m)}{\rho_m} g dt + \int \frac{k(\rho_e - \bar{\rho})}{\rho_m} dt = u_{y1}' + u_{y2}' \tag{9}$$

Therefore

$$u_{y1}' = \int \left(\frac{\rho_e}{\rho_m} - 1 \right) g dt = \int \frac{\Delta T_m}{\Delta T_0} \frac{\Delta T_0}{T_e} g dt \tag{10}$$

where T_e is the indoor (environment) air temperature (°C), T_0 is the cold air temperature (°C), T_m is the axis temperature of the cold air jet (°C), $\Delta T_0 = T_0 - T_e$, and $\Delta T_m = T_m - T_e$.

Substituting the pivot temperature with the pivot velocity, the last equation can be expressed as

$$u_{y1}' = \int \frac{\Delta T_m}{\Delta T_0} \frac{\Delta T_0}{T_e} g dt = 0.73 g \int \left(\frac{v_m}{v_0} \right) \frac{\Delta T_0}{T_e} \frac{ds}{v_m} \tag{11}$$

where v_m is the jet centerline velocity (m/s) and v_0 is the nozzle exit velocity (m/s).

So

$$u_{y1}' = 0.73 g \frac{\Delta T_0}{v_0 T_e} s \tag{12}$$

Similarly

$$u_{y2}' = k \left(1 - \frac{\bar{\rho}}{\rho_e} \right)$$
$$\left[0.73 g \frac{\Delta T_0}{v_0 T_e} s + \frac{1}{0.48 v_0} \left(\frac{as^2}{2d_0} + 0.147 s \right) \right] \tag{13}$$

Combining equations (12) and (13) gives the pivot velocity of the cold jet

$$u_y' = 0.73 g \frac{\Delta T_0}{v_0 T_e} s + k \left(1 - \frac{\bar{\rho}}{\rho_e} \right)$$
$$\left[0.73 g \frac{\Delta T_0}{v_0 T_e} s + \frac{1}{0.48 v_0} \left(\frac{as^2}{2d_0} + 0.147 s \right) \right] \tag{14}$$

The descent distance of the cold jet pivot in the vertical direction is

$$y' = \int u_y' dt$$
$$= \int 0.73 g \frac{\Delta T_0}{v_0 T_e} s dt + \int k \left(1 - \frac{\bar{\rho}}{\rho_e} \right)$$
$$\left[0.73 g \frac{\Delta T_0}{v_0 T_e} s + \frac{1}{0.48 v_0} \left(\frac{as^2}{2d_0} + 0.147 s \right) \right] dt = y_1' + y_2'$$
$$\tag{15}$$

According to fluid mechanics[19]

$$y_1' = \frac{0.73 g}{0.48 v_0^2} \frac{\Delta T_0}{T_e} \left(\frac{as^3}{3d_0} + \frac{0.147}{2} s^2 \right)$$
$$= \frac{g \Delta T_0}{v_0^2 T_e} \left(0.51 \frac{as^3}{d_0} + 0.35 s^2 \right) \tag{16}$$

The integral of y_2' times s is

$$y_2' = k \left(1 - \frac{\bar{\rho}}{\rho_e} \right) \left[0.73 g \frac{\Delta T_0}{v_0 T_e} \frac{1}{0.48 v_0} \left(\frac{as^3}{3d_0} + \frac{0.147 s^2}{2} \right) \right.$$
$$\left. + \frac{1}{(0.48 v_0)^2} \times \frac{1}{2} \left(\frac{as^2}{2d_0} + 0.147 s \right)^2 \right] \tag{17}$$

Substituting y_1' and y_2' into equation (15) and simplifying give

$$y' = \frac{g \Delta T_0}{v_0^2 T_e} \left(0.51 \frac{as^3}{d_0} + 0.35 s^2 \right) + k \left(1 - \frac{\bar{\rho}}{\rho_e} \right)$$
$$\left[\frac{g \Delta T_0}{v_0^2 T_e} \left(0.51 \frac{as^3}{d_0} + 0.35 s^2 \right) + \frac{2.17}{v_0^2} \left(\frac{as^2}{2d_0} + 0.147 s \right)^2 \right]$$
$$\tag{18}$$

Equation (18) gives the change in the jet pivot descent distance as a function of the horizontal distance s. Dividing y' by the nozzle's diameter d_0 gives a dimensionless expression

$$\frac{y'}{d_0} = \frac{g d_0 \Delta T_0}{v_0^2 T_e} \frac{s^2}{d_0^2} \left(0.51 \frac{as}{d_0} + 0.35 \right) + k \left(1 - \frac{\bar{\rho}}{\rho_e} \right)$$
$$\left[\frac{g d_0 \Delta T_0}{v_0^2 T_e} \frac{s^2}{d_0^2} \left(0.51 \frac{as}{d_0} + 0.35 \right) + \frac{2.17}{d_0 v_0^2} \left(\frac{as^2}{2d_0} + 0.147 s \right)^2 \right]$$
$$\tag{19}$$

Introducing the Archimedes number $Ar = g d_0 \Delta T_0 / v_0^2 T_e$, equation (19) is transformed into

$$\frac{y'}{d_0} = Ar \left(\frac{s}{d_0} \right)^2 \left(0.51 \frac{as}{d_0} + 0.35 \right) \left[1 + k \left(1 - \frac{\bar{\rho}}{\rho_e} \right) \right]$$
$$+ \frac{2.17 k (1 - \bar{\rho}/\rho_e)}{d_0 v_0^2} \left(\frac{as^2}{2d_0} + 0.147 s \right)^2 \tag{20}$$

Equation (20) is the final dimensionless path equation for a horizontal jet in an air-conditioned space subjected to a plume.

Effect of several plumes

Equation for the jet with two equal plumes $Q_1 = Q_2$. Assume that the two plumes have the same heat power, $Q_1 = Q_2$, that the distance between them is x_0 and the mixing height is z_m. Equation (3) gives the density of the plume after the two equally powerful plumes are mixed.

Thus, the dimensionless equation for the jet subject to the effects of the two plumes is

$$\frac{y'}{d_0} = \text{Ar}\frac{s^2}{d_0^2}\left(0.51\frac{as}{d_0} + 0.35\right) + k\left(1 - \frac{\bar{\rho}}{\rho_e}\right)$$

$$\left[\text{Ar}\frac{s^2}{d_0^2}\left(0.51\frac{as}{d_0} + 0.35\right) + \frac{2.17}{d_0 v_0^2}\left(\frac{as^2}{2d_0} + 0.147s\right)^2\right] \quad (21)$$

where the average density of several plumes can be expressed as

$$\bar{\rho} = \frac{1}{z - z_m}\int_{z_m}^{z}\rho_e\frac{2\left(\frac{5F}{4\alpha}\right)^{1/3}\left(\frac{6\alpha z_m}{5}\right)^{5/3}g}{2\left(\frac{5F}{4\alpha}\right)^{1/3}\left(\frac{6\alpha z_m}{5}\right)^{5/3}g + 2F}dz \quad (22)$$

Equation for the jet with two plumes of different power $Q_1 \neq Q_2$. If the two plumes have different power, $Q_1 \neq Q_2$, the distance between them is x_0, the mixing height is z_m, and the buoyancy flux ratio is ψ; equation (4) gives the density of the plume after they mix. Thus, the dimensionless equation for the jet now has the same form as equation (21)

$$\frac{y'}{d_0} = \text{Ar}\frac{s^2}{d_0^2}\left(0.51\frac{as}{d_0} + 0.35\right) + k\left(1 - \frac{\bar{\rho}}{\rho_e}\right)$$

$$\left[\text{Ar}\frac{s^2}{d_0^2}\left(0.51\frac{as}{d_0} + 0.35\right) + \frac{2.17}{d_0 v_0^2}\left(\frac{as^2}{2d_0} + 0.147s\right)^2\right] \quad (23)$$

where the average density of several plumes can be expressed as

$$\bar{\rho} = \frac{1}{z - z_m}\int_{z_m}^{z}\rho_e\frac{\left(1 + \psi^{1/3}\right)\left(\frac{5F_1}{4\alpha}\right)^{1/3}\left(\frac{6\alpha z_m}{5}\right)^{5/3}g}{\left(1 + \psi^{1/3}\right)\left(\frac{5F_1}{4\alpha}\right)^{1/3}\left(\frac{6\alpha z_m}{5}\right)^{5/3}g + (1 + \psi)F_1}dz \quad (24)$$

Test measurements

The schematic of the environmental laboratory building and air-conditioning system layout is shown in Figure 2. The laboratory air-conditioning system ensures the sent key air temperature and velocity, and ensures that the jet interferes in other motions, such as infiltration air movement and the envelope structure heat transfer.

The model was evaluated using test room experiments. The dimensions of the test room were length 5 m, width 3.5 m, and height 2.5 m. The heat source for the plumes was a convector heater, capable of creating a heat flow of up to 1000 W.

The thermal plume is composed of lawn lamp, as the simulation of point source plume. The lamp shade
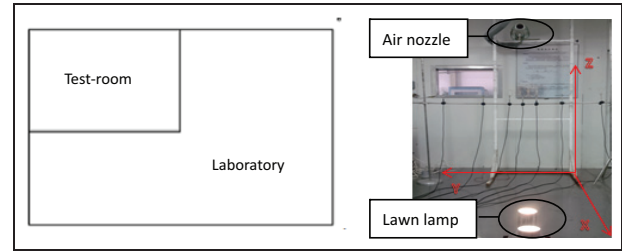

Figure 2. Structure of building environmental laboratory schematic and air conditioning system layout.

needs to be increased to fix the lawn, as shown in Figure 3. Change the different power of tubes to satisfy the requirements of plume heat source. In order to ensure to match the motion feature of point source plume, the jet radius of lawn lamp b and flow height x should meet the requirements of equation (25) and the entrainment coefficient $\alpha = 0.09$. According to calculations of equation (25), $b = 30$ mm and $x = 300$ mm

$$b = \frac{6}{5}\alpha x \quad (25)$$

One air supply nozzle with a diameter of 0.6 m was located close to the middle of the shorter wall of the test room at a height of 1.6 m. Venturi was used as the air supply nozzle. The design of venturi tube is divided into five parts: the entrance section A, the conical contraction section B, the cylindrical throat section C, the design of inner diameter D, and the diffusion section E. The size of each part and the cone angle are shown in Figure 4. From the figure, the diameter of A is the same as the design of the pipeline inner diameter D; entrance length is two times the design of inner diameter; the throat diameter $d = 0.62 \times$ D; and the diffusion section of the minimum end diameter is equal to the throat diameter d and the maximum end diameter is equal to the design of diameter D. The jet nozzle in the experiments of venturi tube simulation prototype has certain practicality.

The experimental conditions are shown in Table 1. An anemometer was used to measure the velocity of the air, and thermocouples were adopted to measure the temperatures of the environment and the air supply. The model experiment uses Delta OHE universal wind instrument made in Italy, and the basic parameters are shown in Table 2.

There were, in total, 924 measuring points recorded for each experimental condition used in Figure 5. The x–y plane lies in the laboratory floor, while z is in the altitude direction of the laboratory. A total of 12 horizontal measuring rows were arranged in the vertical direction from a height of 0.5 m to the nozzle height (1.6 m) at equal intervals (0.1 m). Each measuring row included seven measuring points at different intervals
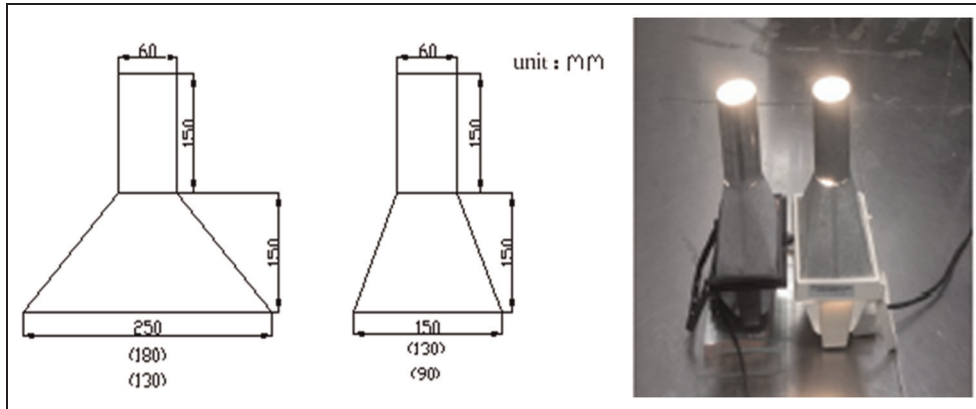
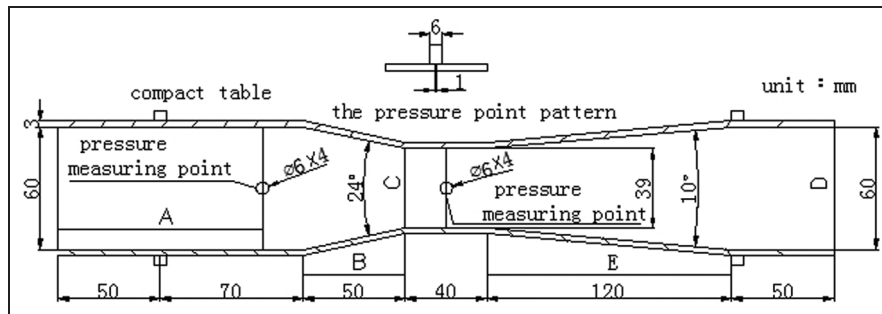**Figure 3.** Front view and side view of lawn lamp shade structure.

Figure 4. The design dimensions of venturi tube.

Table 1. Experiment conditions.

		Supply air jet height (m)	Supply air velocity (m/s)	Heat source number/power (w)	Distance between plumes (m)	Supply air temperature (°C)	Indoor air temperature (°C)
Plumes with same power	Case1	1.6	2	2/150,150	0.1	20	26
	Case 2	1.6	2	2/300,300	0.1	20	26
	Case 3	1.6	2	2/500,500	0.1	20	26
Plumes with different power	Case 4	1.6	2	2/100,300	0.1	20	26
	Case 5	1.6	2	2/100,500	0.1	20	26
	Case 6	1.6	2	2/300,500	0.1	20	26
	Case 7	1.6	2	2/150,1000	0.1	20	26

Table 2. Delta OHE universal anemometer.

The main parameters of Delta OHE universal anemometer wind speed probe	
Wind speed measuring range	0–5 m/s
Measurement precision	± 0.01 m/s
Working temperature	−20°C–50°C
Working voltage	220 V

(0.3, 0.2, 0.1, 0.1, 0.2, and 0.3 m, respectively) in the *y*-direction. The choice of different intervals is mainly in response to the rapidly changing velocity gradient around the pivot. The measuring points in the *x*-direction are at intervals of 0.3 m and are 11 in total.

First, testers arrange the seven universal anemometers with unequal spacing of *Y*-direction on air vents' horizontal distance of 0 positions. Second, they arrange mobile test position every 10 cm along the height direction (*Z*-direction) and complete 84 measuring points in the region. Third, they measure every 30 cm along the *X*-direction to the next test area, and so on, until all the 924 points are measured.
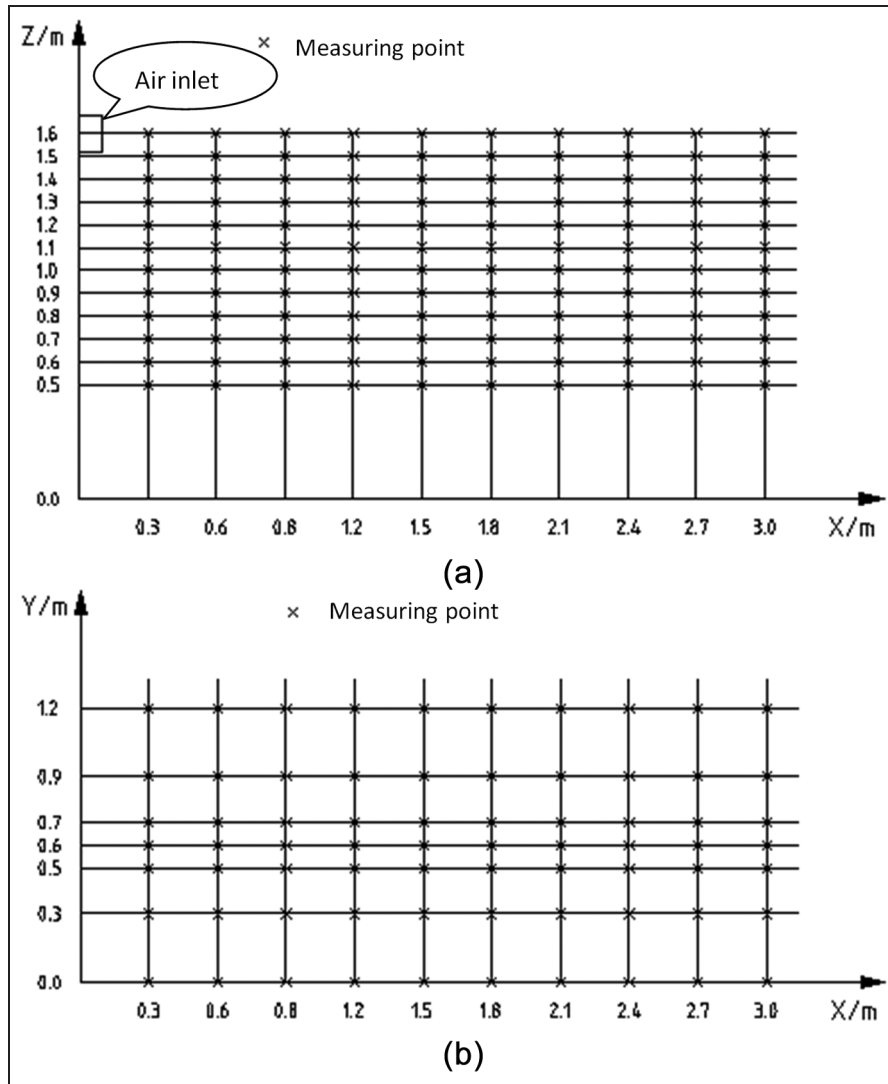
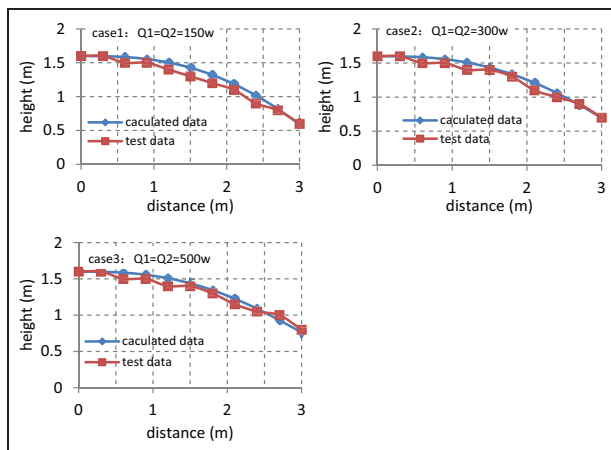**Figure 5.** Layout of measuring point coordinates.

Figure 6. Comparison between theoretical analysis and experiment data with cases 1–3.

In order to ensure the accuracy of the experiment, each measuring point, every 1 min a group of data, records a total of three sets of data, and the average value is taken as the test data of the measuring point. Replace the lawn lamp source for other conditions during the experiment, need to readjust heater position, to ensure that the indoor temperature stabilizes at 26°C, then measure these measuring points.

Results

Two plumes with the same power

The experimental results and corresponding theoretical calculations for the jet under two plumes with the same power are shown in Figure 6. From Figure 5, it can be seen that the experimental values measured using conditions 1–3 are all smaller than the theoretical values. At
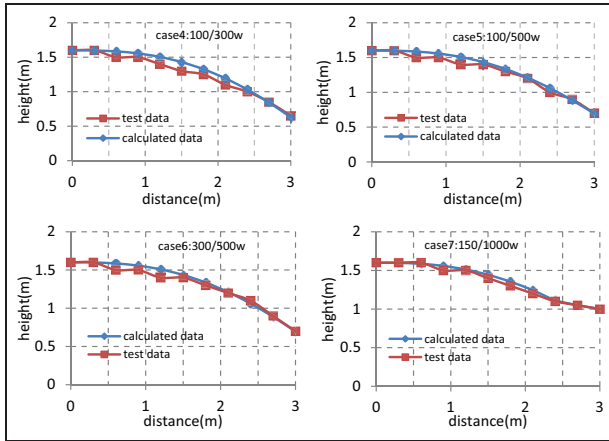
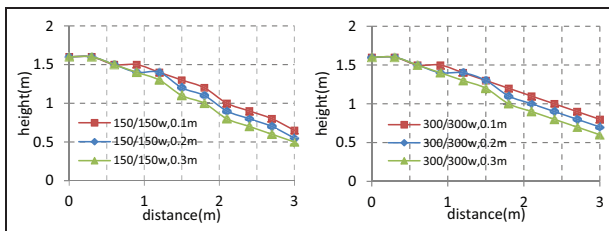**Figure 7.** Comparison between theoretical analysis and experiment data with cases 4–7.

Figure 8. The effects of distance between the two plumes on the non-isothermal air jet.
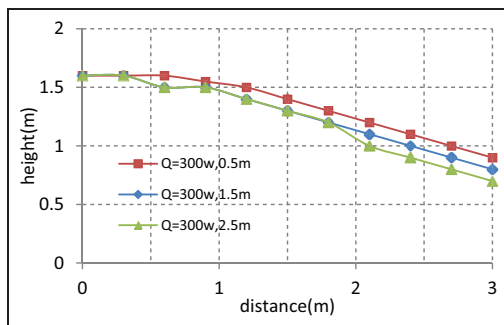

Figure 9. The effects of the location of the plume on the non-isothermal air jet.

$s = 3$ m, the maximum error in the jet curve is within 15%. On the whole, the theoretical values are in good agreement with the experimental values.

Two plumes with different power

The experimental results and theoretical calculations for two plumes with different power are shown in Figure 7. From Figure 6, it can be seen that the experimental values measured using conditions 4–7 are all

smaller than the theoretical values. At $s = 3$ m, the maximum error in the jet curve is within 15%. On the whole, the theoretical values are again in good agreement with the experimental values. Figure 6 shows the comparison between theoretical analysis and experiment data with cases 1–3.

Discussion

Distance between the two plumes

The analysis in the previous section is based on a distance between the plumes of 0.1 m. The experimental and theoretical jet curves when the distance is enlarged to 0.2 and 0.3 m are shown in Figure 8. Under these conditions, the plumes are located symmetrically 1.5 m away from the nozzle.

According to the theoretical analysis, the mixing height of the plumes is $z_m = \lambda_m x_0$, which shows that the distance between the plumes can influence the mixing height. The average density of the air after mixing is $\bar{\rho} = \int_{z_m}^{h} \rho \mathrm{d}h/(h - z_m)$. This shows that as the mixing height increases, the average density from the mixing height z_m to the air supply height h increases, the buoyancy power F_b decreases, and the descent distance of the jet increases.

From Figure 5, it is seen that the effect of the plumes on the jet curve is largest when the power of the two plumes is 150 W and the distance between the plumes is 0.1 m. The jet curve is raised to the largest degree at $s = 3$ m. Within the range $s = 1.3$–1.5 m, the jet curve is raised more than when $x_0 = 0.2$ m and $x_0 = 0.3$ m. When the power of the heat source is 300 W, the results are the same. The effect of the buoyancy of the plumes on the jet curve appears to decrease as the distance between the plumes increases. Thus, increasing the distance between the plumes can reduce the effect of the plumes on the jet curve.

The locations of the plumes

Figure 9 shows the effect of the plumes on the jet curve for different locations of the plumes. The heat source was located 0.5, 1.5, and 2.5 m from the nozzles successively while keeping the heat source power constant at 300 W. From the results, it can be seen that the coupling effect first occurs when the heat source is 0.5 m from the jet. The plume begins to influence the jet at 0.5 m height and the jet curve is lifted. However, the jet has a high velocity and strong rigidity, and so the effect on the plume is not distinct. When the heat source is located 1.5 m from the nozzles, the plumes and the jet start to interact at $s = 1.5$ m and the jet curve begins to migrate. In general, at $s = 3$ m, the conditions having the plume at 0.5 m from the nozzle influence the jet
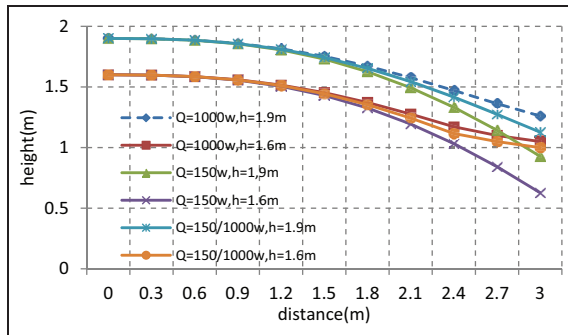
Figure 10. The effect of the plumes on the jet curve under conditions of different air supply heights.
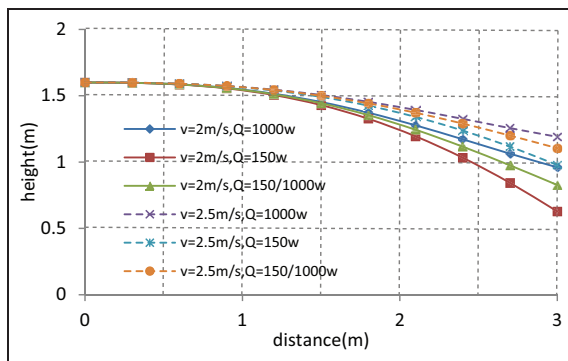

Figure 11. The effect of the plume on the jet curve under the conditions of different air supply velocities.

curve most. This is due to the long interaction time within which the jet curve can be affected.

The air supply height of the jet

Figure 10 shows the effect of the air supply height on the jet curve. It can be seen that when $h = 1.9$ m and $h = 1.6$ m, the effect on the jet curve increases if the heating power is increased from 150 to 1000 W. The greater the heating power, the more evident is the effect. Also, the extent of the effect of two plumes with different power is right between the effects of two single plumes. When the air supply height is 1.9 m and the heat source power is 1000 W, the trend in the jet curve is downward. This means that the buoyancy of the plumes cannot change the tendency of the jet. When the air supply height is 1.6 m and the heat source power increases from 150 to 1000 W, the tendency of the jet to bend upward is fairly apparent. At $s = 3$ m, the jet curve is raised approximately 0.6 m by the buoyancy of the plumes. It is clear that the air supply height influences the jet curve the most. The effect of the plumes on the jet curve can be reduced by increasing the height difference between the cold jet and the

hot plumes. This can also be confirmed from the experiments.

The air supply velocity of the jet

Figure 11 shows the effect of the air supply velocity on the jet curve. From the figure, it is seen that if the air supply height is 1.6 m and the air supply velocity is 2 m/ s, the jet curve is raised at $s = 1.5$ m when the heat source power increases from 150 to 1000 W. The lifting is also evident at $s = 3$ m. If the air supply velocity is increased to 2.5 m/s, then increasing the heating power lifts the jet curve at the same time. However, the amount of lift at $s = 3$ m/s under these conditions is smaller than when the velocity was 2 m/s. This is because increasing the velocity of the air supply increases the rigidity of the jet and the buoyancy of the plume is relatively weakened. Thus, the effect of the plume on the jet curve is reduced. The above phenomenon is also observed when two plumes with different power are used. It is apparent that when the velocity of the air supply increases, the interference caused by the plumes can be reduced.

Conclusion

This article presents a theoretical and experimental study of the interaction between a plume and an air jet. In the study, the behavior of the (non-isothermal) air jet is affected by the plume which rises from a point heat source due to buoyancy. A theoretical model, which can predict the flowing action of the non-isothermal air jet, was developed. It is based on the theory of a pure plume and also incorporates the effect of the plume generated by the buoyancy of the source. It is concluded that the interaction between the air jet and the plume has an effect on the trajectory of the non-isothermal air jet. The trajectory is mainly determined by the jet height, the jet angle, and the velocity of the supplied air. The buoyancy source's efforts to baffle the descent of the cold air have even been effective in reversing the direction of the trajectory. This generalization is predicted by the theoretical model and is well supported by the field experiments. Further investigations of the effects of the buoyancy force and jet force should be carried out, perhaps, to more thoroughly determine the effects of the plumes.

References

1. Hagstrom K and Sandberg E. Classification for the room air conditioning strategies. *Build Environ* 2000; 35(8): 699–707.
2. Zhou MR. *Fluid mechanics, pumps and fans*. Woodstock: CAB Press, 1996.
3. Gu X, Han W, Zhao J, et al. Calculation method of nozzle jets in large space. *Heat Vent Air Cond* 2009; 39: 128–136.
4. Quyang Q, Dai W, Li H, et al. Study on dynamic characteristics of natural and mechanical wind in built environment using spectral analysis. *Build Environ* 2006; 41: 418–426.
5. Song G. *Visualization of the airflow patterns of 12 typical diffusers and experimental investigation on the turbulent coefficient*. China: Xi'an University of Architecture and Technology, 2005.
6. Gao J, Li X and Gao F. Coincidence and entrainment of air jets of the stratified air conditioning in large spaces. *J Harbin Inst Technol* 2004; 36: 815–818.
7. Zeldovich YB. The asymptotic laws of freely-ascending convective flows. *Zh Eksp Teor Fiz* 1937; 7: 1463–1465.
8. Batchelor GK. Heat convection and buoyancy effects in fluids. *Q J Roy Meteor Soc* 1954; 80: 339–358.
9. Morton BR, Taylor G and Turner JS. Turbulent gravitational convection from maintained and instantaneous sources. *P Roy Soc Lond A Mat* 1956; 234: 1–23.
10. Turner JS. Jets and plumes with negative or reversing buoyancy. *J Fluid Mech* 1966; 26: 779–792.
11. Rooney GG and Linden PF. Similarity considerations for non-Boussinesq plumes in an unstratified environment. *J Fluid Mech* 1996; 26: 779–792.
12. Hunt GR and Kaye NB. Lazy plumes. *J Fluid Mech* 1995; 533: 329–338.
13. Batchelor GK, Moffatt HK and Worster MG. *Perspectives in fluid dynamics: a collective introduction to current research*. Cambridge: Cambridge University Press, pp.289–345, 2011.
14. Kaye NB. Turbulent plumes in stratified environments: a review of recent work. *Atmos Ocean* 2008; 46: 433–441.
15. Woods AW. Turbulent plumes in nature. *Annu Rev Fluid Mech* 2010; 42: 391–412.
16. Cooper P and Hunt GR. The ventilated filling box containing a vertically distributed source of buoyancy. *J Fluid Mech* 2010; 646: 39–58.
17. Scase MM, Caulfield CP, Dalziel SB, et al. Time-dependent plumes and jets with decreasing source strengths. *J Fluid Mech* 2006; 563: 443–461.
18. Kaye NG. *Interaction of turbulent plumes*. Cambridge: Department of Applied Mathematics and Theoretical Physics, University of Cambridge, 1998.
19. Gaskin SJ, Papps DA and Wood IR. The axisymmetric equations for a buoyant jet in across flow. In: *Twelfth Australasian fluid mechanics conference* (ed RW Bilger), Sydney, NSW, Australia, 10–15 December 1995, pp. 347–350.
20. Kaye NB and Linden PF. Coalescing axisymmetric turbulent plumes. *J Fluid Mech* 2004; 502: 41–63.
21. Linden PF, Lane-Serff GF and Smeed DA. Emptying filling spaces: the fluid mechanics of natural ventilation. *J Fluid Mech* 1990; 212(1): 309–335.
22. Baines WD and Turner JS. Turbulent buoyant convection from a source in a confined region. *J Fluid Mech* 1969; 37: 51–80.
23. Economidou M and Hunt G. Density stratified environments: the double-tank method. *Exp Fluids* 2009; 46: 453–466.
24. Csanady GT (ed.). *Turbulent diffusion in the environment*. Dordrecht: Kluwer, 1973.
25. Fernando HJS and Smith DC IV. Vortex structures in geophysical convection. *Eur J Mech B Fluid* 2001; 20: 437–470.
26. Coffey CJ and Hunt GR. The unidirectional emptying box. *J Fluid Mech* 2010; 660: 456–474.
27. Site measurement and analysis of indoor thermal environment in a large space building in typical seasons. In: *2003 HVAC forum in China and Japan*, Shanghai, China, 2003.
28. Linden PF and Cooper P. Multiple sources of buoyancy in a naturally ventilated enclosure. *J Fluid Mech* 1996; 311: 177–192.
29. Hunt GR. Time-dependent displacement ventilation caused by variations in internal heat gains: application to a lecture theatre. *In: Proceedings of ROOMVENT '98 conference*, Stockholm, Sweden, 14–17 June 1998, pp.203–210.
30. Hunt GR. Classical plume theory: 1937-2001 and beyond. *IMA J Appl Math* 2011; 76: 424–448.
31. Chen ZD, Li Y and Mahoney J. Natural ventilation in an enclosure induced by a heat source distributed uniformly over a vertical wall. *Build Environ* 2001; 36: 493–501.
32. Hunt GR, Cooper P and Linden PF. Thermal stratification produced by plumes and jets in enclosed spaces. *Build Environ* 2001; 36: 871–882.
33. Cho Y and Awbi HB. A study of the effect of heat source location in a ventilated room using multiple regression analysis. *Build Environ* 2007; 42: 2072–2082.
34. List EJ. Turbulent jets and plumes. *Annu Rev Fluid Mech* 1982; 14: 189–212.